Conductance of quantum waveguides with a rough boundary

1992 J. Phys.: Condens. Matter 4 10421

(http://iopscience.iop.org/0953-8984/4/50/030)

J. Phys.: Condens. Matter 4 (1992) 10421–10432. Printed in the UK

Conductance of quantum waveguides with a rough boundary

Y Takagaki and D K Ferry

Center for Solid State Electronics Research, Arizona State University, Tempe, AZ 85287-6206, USA

Received 6 August 1992

Abstract. A quantum mechanical calculation of the conductance of quantum wires in the presence of boundary scattering is presented. The scattering-matrix method is used to evaluate the transmission coefficients through electron waveguides with a random fluctuation in the local width of the channel. The conductance quantization of ballistic wires breaks down for strong disorder. We find that the conductance has a dip when a new propagating mode opens. The conductance is suppressed exponentially as the length of the wire is increased, demonstrating localization of electron states in the quasi-one-dimensional system. The dependences of the localization length on the parameters of the wires are examined. The probability distribution of the conductance due to coherent scattering from the rough boundary is found to possess a long tail.

1. Introduction

Low-temperature transport properties of an electron in low-dimensional systems have attracted much attention in recent years [1]. In the Drude model, an electron is assumed to move along a classical trajectory between independent scattering events. The probability of the electron undergoing collisions with scatterers is evaluated by taking an average over disorder, i.e., it depends on the density of impurities. This is no longer valid, however, if interference of scattering from different impurities is not negligible. The interference between the various Feynman trajectories gives rise to a variety of quantum interference phenomena [2]. If the sample dimensions are less than the phase coherence length of an electron, the conductance is no longer a self-averaged quantity and possesses a fluctuation with the universal amplitude $\sim e^2/h$ among different (but macroscopically the same) samples [3]. In this regime, the conductance depends critically on the specific impurity configuration in the sample [2, 3].

In narrow channels created in a high-mobility two-dimensional electron gas (2DEG), electrons can transit the entire device without being scattered by their parent donors. We may expect that the scattering from an inhomogeneous boundary plays a fundamental part in the transport properties in the nearly perfect conductors. The size effects have been extensively studied in metal films. The resistivity increases rapidly as the film thickness is reduced below the elastic mean free path l_e [4]. Similar effects are expected in the wires. It is important to note that the Fermi wavelength λ_F of electrons in semiconductors is much larger than that in metals, and hence only a small number of modes are occupied below the Fermi energy, and the discrete energy-level spectrum needs to be taken explicitly into account [5]. The resistivity of

0953-8984/92/5010421+12$07.50

the one-dimensional (1D) semiconductor systems would be an interesting subject since a high-mobility effect, on the other hand, has been predicted because of suppression of impurity scattering [6]. There are several nanofabrication technologies to realize narrow GaAs–AlGaAs wires, where a variety of ballistic transport phenomena have been observed [1]. However, the experiment to investigate the size effects in the GaAs–AlGaAs wires is not easy. Under the present technology, the confinement potential is usually imposed by depletion methods utilizing such techniques as split-gate [7], shallow etching [8] and focused-ion-beam implantation [9]. In these devices, the edge potential is nearly parabolic [10] rather than a hard-wall confinement created by the conduction band discontinuity. Therefore, it is considerably difficult to estimate the precise conduction width [11]. The methods utilizing selective crystal growth techniques [12] can provide the accurate channel width. Unfortunately, the quality of the grown material is not yet sufficient to observe the ballistic effects.

The effect of the rough boundary in the GaAs–AlGaAs wires was first reported by Thornton *et al* [13]. They have investigated low-field positive magnetoresistance phenomena and found that, even though the channel boundary is predominantly specular [14], a small amount of non-specular boundary reflection gives rise to a peak at a field value which results in the cyclotron diameter being comparable with the channel width and hence causes electrons to collide frequently with the boundary [13, 15]. This mechanism is based on the classical scattering from the boundary. Our interest is raised to the effects of coherent boundary scattering. Quantum interference of an electron wave scattered from the non-uniform boundary will lead to the localization of electron states [16].

The purpose of this paper is to present results of numerical simulation of the quantum transport through narrow wires in the presence of the boundary roughness scattering. The non-uniform quantum waveguide is decomposed into uniform waveguide sections. A mode-matching is then made across the boundary between the sections. The transmission coefficients are obtained by cascading matrices which characterize each junction. We utilize the scattering matrix method to evaluate the overall transmission. This method was used by Cahay *et al* [17, 18] to study the conductance of disordered systems, where a large number of impurities are embedded in the sample.

2. Numerical model

Consider an infinite strip containing a finite scattering region. We model the boundary fluctuation in the scattering region as illustrated in figure 1. An electron waveguide with a non-uniform width defined by $y_2(x)-y_1(x)$ is terminated by perfect leads with uniform width W. The wire structure is divided lengthwise into a few sections. An equivalent length d is assigned for all waveguide sections. The width in each section is assumed to be uniform. In real devices, $y_1(x)$ and $y_2(x)$ are smooth functions of the coordinate. The randomness in $y_1(x)$ and $y_2(x)$ is conventionally assumed to be Gaussian for analytical treatment. Our model can simulate the arbitrary boundary contour if d is chosen sufficiently small compared to λ_F. However, we make the following assumption, for simplicity. We introduce a deviation in the local width of the wire from an average W by putting $y_1 = w_1$ and $y_2 = W + w_2$, where w_1 and w_2 are distributed uniformly between $-\Delta/2$ and $\Delta/2$. Therefore, the deviations

give the correlation function

$$\langle w_1(x)\rangle = \langle w_2(x)\rangle = \langle w_1(x)w_2(x')\rangle = 0 \tag{1a}$$

$$\langle w_1(x)w_1(x')\rangle = \langle w_2(x)w_2(x')\rangle = \begin{cases} \dfrac{\Delta^2}{12}\dfrac{d-|x-x'|}{d} & |x-x'|<d \\ 0 & |x-x'|>d. \end{cases} \tag{1b}$$

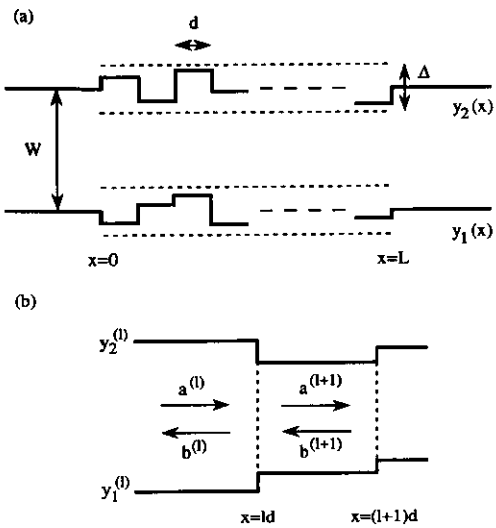

Figure 1. Schematic view of an electron waveguide with an inhomogeneous boundary. In each waveguide section with length d, the width is assumed to be uniform.

If $d \ll \lambda_F$, the fluctuation resembles 'white noise'. This may be plausible in metal wires (and GaAs–AlGaAs wires created by means of crystal growth), where the roughness corresponds to physical absence of atoms at the surface (interface between GaAs and AlGaAs). In contrast, in GaAs–AlGaAs wires utilizing the split-gate techniques, the inhomogeneity of the channel width may arise from the random distribution of donors [19]. The correlation length of such roughness is expected to be larger than λ_F since the source of the roughness is several tens nanometers away from 2DEG layer.

3. Scattering-matrix approach

In this section, we describe the numerical technique, which is based on the mode-matching method and the scattering matrix method, to evaluate the transmission coefficients through the inhomogeneous wire.

The wavefunction in the lth waveguide section $[(l-1)d < x < ld, y_1^{(l)} < y < y_2^{(l)}]$ is given in terms of the modal expansion

$$\Phi(x,y) = \sum_j^M (k_j^{(l)})^{-1/2}[a_j^{(l)}\exp(ik_j^{(l)}(x-(l-1)d)) + b_j^{(l)}\exp(-ik_j^{(l)}(x-ld))]u_j^{(l)}(y). \tag{2}$$

Assuming hard-wall confinement in the transverse direction, the orthonormalized functions in the y direction $u_j(y)$ and the longitudinal wavenumbers k_j are given by, respectively

$$u_j^{(l)}(y) = \sqrt{2/(y_2^{(l)} - y_1^{(l)})}\sin[[j\pi/(y_2^{(l)} - y_1^{(l)})](y - y_1^{(l)})] \tag{3}$$

$$k_j^{(l)} = \sqrt{[2m E_F/\hbar^2 - [j\pi/(y_2^{(l)} - y_1^{(l)})]^2]} \tag{4}$$

where $E_F = \hbar^2 k_F^2/2m$ is the Fermi energy of electrons. The value M is a practical cut-off. It is important in the quantum mechanical calculation to include evanescent modes, for which k_j are imaginary, since the coupling through the evanescent modes is not negligible [20].

For each junction between adjacent waveguide sections, a scattering matrix is determined which relates the amplitudes of the incoming and outgoing states. We define the scattering matrices $\mathbf{S}_l$ associated with the junction at $x = ld$ as [21]

$$\begin{bmatrix} a^{(l+1)} \\ b^{(l)} \end{bmatrix} = \mathbf{S}_l \begin{bmatrix} a^{(l)} \\ b^{(l+1)} \end{bmatrix} = \begin{bmatrix} \mathbf{t}' & \mathbf{r} \\ \mathbf{r}' & \mathbf{t} \end{bmatrix} \begin{bmatrix} a^{(l)} \\ b^{(l+1)} \end{bmatrix} \tag{5}$$

where $a^{(i)}$ and $b^{(i)}$ are column vectors representing the amplitude of modes. The $M \times M$ matrices $\mathbf{t}$, $\mathbf{r}'$, $\mathbf{r}$, and $\mathbf{t}'$ describe mode-mixing properties across the junction. The exact analytical form of the scattering matrix is derived in the appendix. These matrices are cascaded to yield the overall scattering matrix for the entire structure [7]

$$\mathbf{S} = \mathbf{S}_0 \otimes \mathbf{S}_1 \otimes \mathbf{S}_2 \ldots . \tag{6}$$

The reason that we use the scattering matrix method is its numerical stability. For comparison, the transfer matrix method is one of the most convenient ways to evaluate the transmission coefficients through composite systems because of its simplicity. However, it is numerically unstable when dealing with structures large compared to the de Broglie wavelength. In the transfer matrix, the amplitudes of modes in the right-hand side are evaluated relative to those in the left-hand side. If we include evanescent modes, the amplitudes, on one hand, decrease exponentially for right-moving evanescent modes. On the other hand, they increase exponentially for the left-moving evanescent modes. Therefore, the transfer matrix methods are not applicable to a problem in which the scattering region is several orders of magnitude longer than the wavelength. In the scattering matrix, however, the amplitudes of outgoing modes are evaluated relative to those of incoming modes. The amplitudes always decrease after the mode-matching procedure and hence the contributions from higher-lying evanescent modes eventually disappear in the overall scattering matrix.

The conductance of the sample is given from the overall scattering matrix through the Landauer formula [22]. There are several versions of the conductance formula depending on the geometry of the leads. We use the multichannel version of the two-terminal Landauer formula in which the phase coherence is constrained to the wire length:

$$G = (2e^2/h)\,\mathrm{Tr}[\mathbf{t}\mathbf{t}^\dagger]. \tag{7}$$

Here the trace is defined to operate only over the propagating modes. It has been found that the $\ln|\mathbf{t}|^2$ is an appropriate scaling variable in the localized regime [23].

4. Results and discussion

In this section we present the numerical results, which consist of two parts: (i) the energy dependence of the conductance in order to study the effects of the boundary scattering on the conductance quantization and (ii) the length dependence of the conductance in order to study localization effects in quasi-1D system. We take $M = 50$ modes into account in the calculation. It is possible to include more modes in the simulation. However, contributions from the higher-lying evanescent modes are negligible when a sufficient number of lower-lying modes are taken into account [20].

Figure 2 shows the energy dependence of the conductance of an $L/W = 7$ wire in the presence of the 'white noise' type ($d/W = 0.1$) boundary roughness. For $\Delta = 0$ (perfect wire), the conductance is quantized in units of $2e^2/h$ in steplike fashion and each step corresponds to the opening of a new conducting mode [7]. The number of propagating modes in the perfect leads is given as a truncation to an integer $N = [k_F W/\pi]$. The impurity scattering in the channel has been found to obscure the quantization [24, 25]. The calculated conductance indicates that the quantization can be destroyed by the boundary roughness scattering. The plateau structures are essentially intact for lower energy. The electron states are localized near the propagation thresholds of modes and hence the step structure is shifted to higher energies and is rounded. The universal conductance fluctuations (UCF) [3] are developed when the Fermi energy is increased. The breakdown of the quantized conductance for higher energy is significant if Δ/W is held constant compared to the case of fixed Δ/λ_F. This is because of larger inter-mode coupling for larger Δ/λ_F. We find that dips appear near the thresholds of the subbands. The longitudinal momentum of the barely opened mode is small, so that scattering from all other modes to the localized mode is enhanced [24]. This feature has been observed in the presence of attractive impurities in the wire and is ascribed to the transmission resonances through quasi-bound states [20, 25]. From the results for strong disorder we find that the conductance saturates at higher energies. The conductance due to randomness has been derived by Pichard [26]:

$$g = \frac{G}{2e^2/h} = \sum_{i=1}^{N} \frac{2}{\cosh(2L/\xi_i) + 1} \tag{8}$$

where ξ_i is the decay length of the ith wavefunction and converges towards localization length in the limit $L \to \infty$. The values of $1/\xi_i$ of the disordered system are equally spaced and are roughly given by $1/\xi_i \sim i/Nl_e$ due to level repulsion [27]. For $L > l_e$, only active transmission channels, the number of which is roughly given by $N_{eff} \sim Nl_e/L$, contribute to the conduction [27]. Therefore, the opening of new channels is no longer reflected in the conductance $g \sim N_{eff}$.

Figure 3 shows the length dependence of the conductance for a specific realization of the boundary roughness. One can see that the reflection of electrons from the rough surface is rapidly enhanced as L is increased. When the wire length becomes longer than the elastic mean free path, the UCF are fully developed and dominate the behaviour of the conductance. The fluctuation is not self-averaging, i.e., it does not disappear even if L is further increased. The fluctuations are extremely sensitive to the disorder and the energy. A small change in the boundary roughness or the energy induces a drastic modification of the fluctuation pattern. This indicates that the

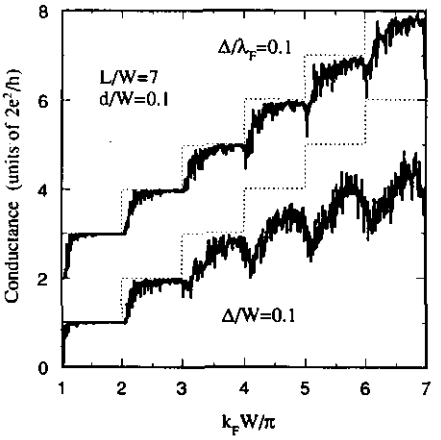

Figure 2. Energy dependence of the conductance of $L/W = 7$ wires. The strength of the boundary roughness is assumed to be $\Delta/W = 0.1$ or $\Delta/\lambda_F = 0.1$. The dotted lines represent the conductance of a perfect wire. The upper curves are offset by $2 \times 2e^2/h$.

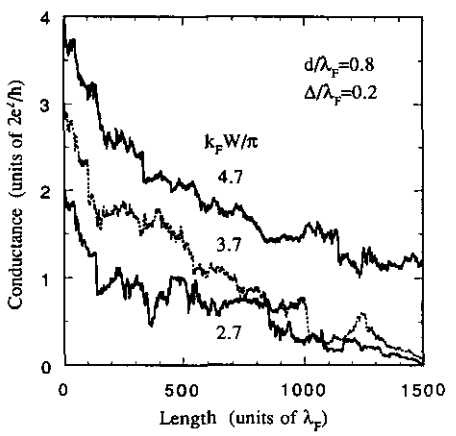

Figure 3. Conductance of inhomogeneous wires as a function of the wire length for $k_F W/\pi = 2.7$, 3.7, and 4.7. The same realization of the boundary roughness is assumed.

conductance fluctuation arises not from classical scattering from the rough boundary but from quantum mechanical phase modulation due to multiple reflections in the wire.

Next, we investigate the conductance ensemble averaged over about 25 equivalent wire samples to eliminate the sample-dependent fluctuations. We find that the averaging process eliminates most of UCF and the averaged conductance decreases monotonically with increasing L. The conductance fluctuations are sensitive to the energy such that the averaging can easily be realized experimentally at finite temperatures if $k_B T$ is larger than $\hbar D/WL$ with D being the diffusion constant of electrons. In figure 4, we show the length dependence of the normalized conductance $g_{\text{norm}} = g/N$. The solid and dotted lines represent averages in terms of $\langle \ln(G) \rangle$

and $\ln(\langle G\rangle)$, respectively. These averages do not make appreciable difference if the disorder is weak. In the strongly localized regime, however, the fluctuation is so large that if we take the average as $\langle G\rangle$ the large conductance values dominate the averaging. We will return to this point later. Figures 4(*a*) and 4(*b*) show results for $d/\lambda_F = 0.2$ and 0.8, respectively. The scattering from the boundary becomes quantitatively weak as d is increased. In the limit of large d, the total transmission probability is expected to be quantized and will be determined by the number of propagating modes at the narrowest part of the wire in so far as the transmission resonances through quasi-bound states in the wire are not important (non-additivity of conductances in two-terminal point contacts in series [28]). In figure 4 the roughness is assumed to be $\Delta/\lambda_F = 0.2$, so that the scattering is weak for wide wires ($\Delta/\lambda_F = 0.2$ corresponds to $\Delta/W \approx 0.15$, 0.11, and 0.05 for $k_F W/\pi = 2.7$, 3.7, and 7.7, respectively). The dependence of the averaged conductance $\langle \ln G\rangle$ on the number of propagating modes is shown in figure 5 for $\Delta/W = 0.1$. One can see in this case, on the contrary, the roughness scattering appears to be strong for large $k_F W/\pi$ as expected from the result in figure 2.

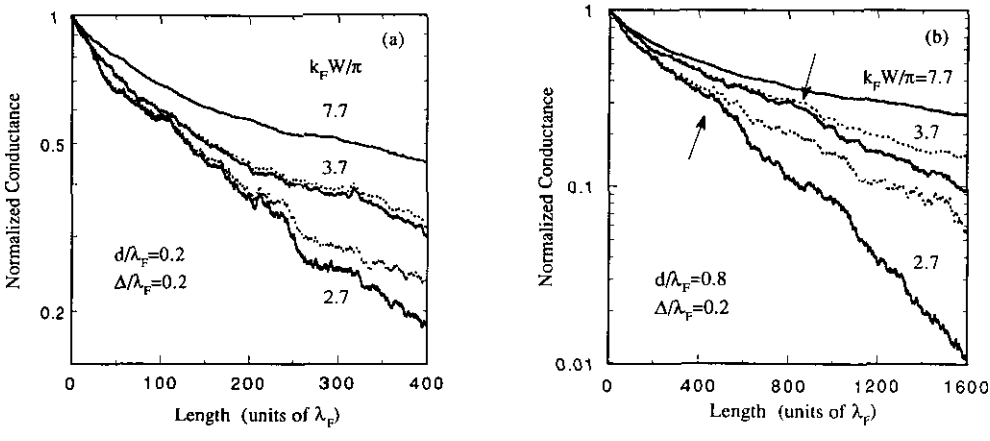

Figure 4. Normalizaed average conductance $G_{av}/(2e^2/h)N$ with N being the number of propagating modes in the perfect leads as a function of the length of the wires. (*a*) The averaged conductance G_{av} is calculated in terms of $\langle \ln G\rangle$ and $\ln\langle G\rangle$ for solid and dotted lines, respectively. (*b*) If the wire length exceeds a critical value indicated by an arrow the conductance decays exponentially.

If only the lowest transverse level is filled, the conductance shows simple exponential dependence on L. An analytical expression for the localization due to boundary roughness has been examined in the one-dimensional case. It has been found that the average value of the conductance depends exponentially on L and all the moments of the conductance are non-self-averaging [16]. With increasing N, an increase in L appears less effective in suppressing the conductance when the wire is relatively short. The non-exponential behaviour of the conductance for larger N may be explained in terms of the multi-subband effect through (8). The numerical results for these wide wires suggest a presence of a critical length L_c as indicated by arrows in figure 4(*b*). This may correspond to a length to achieve $N_{eff} = 1$ (and so

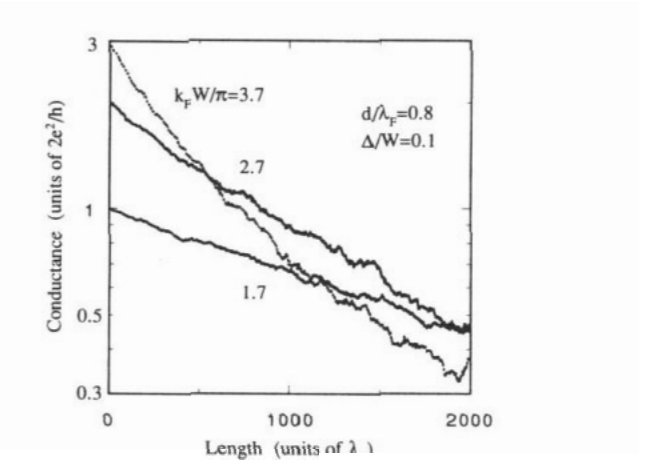

Figure 5. Length dependence of the averaged conductance of inhomogeneous wires when Δ/W is held constant.

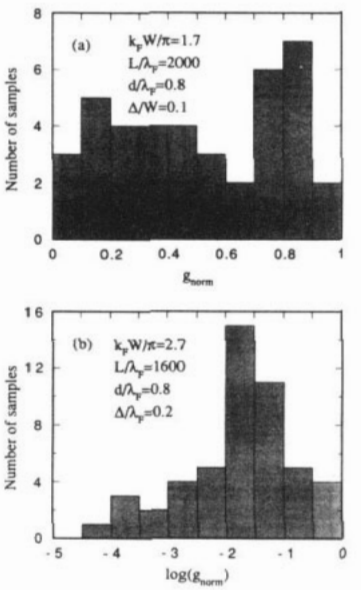

Figure 6. Distribution of the conductance values in (*a*) weakly and (*b*) strongly localized regime.

we expect $g(L = L_c) \sim 1$). If the length exceeds the critical value, the conductance recovers the exponential dependence governed by the ξ_i of the final active channel.

Finally, we focus our attention on the statistical properties of the conductance fluctuations. Figure 6 shows the distribution of G in the weakly localized regime ($(g_{\text{norm}})_{\text{av}} \sim 0.4$) and that of $\log(G)$ in the strongly localized regime ($(g_{\text{norm}})_{\text{av}} \sim 0.01$). We find that the distribution of the conductance possesses long tails which are responsible for the peculiar dependence on various averaging processes. One can see

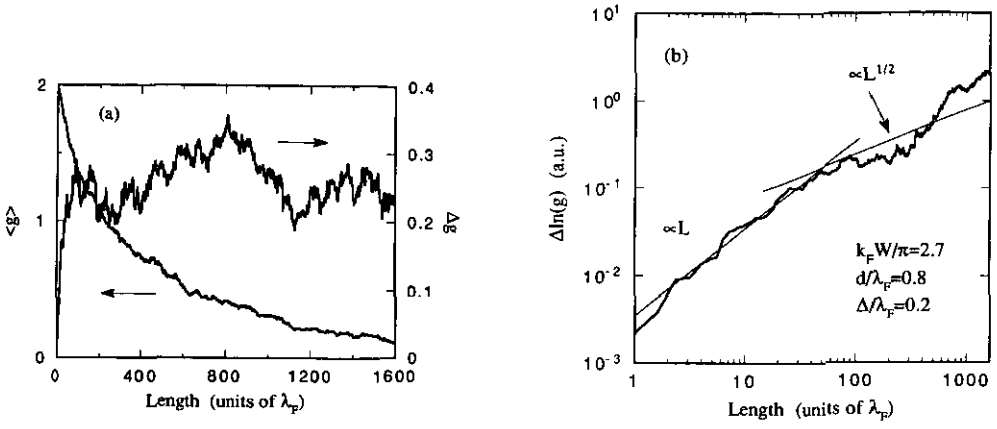

Figure 7. (*a*) The average of the conductance $\langle g \rangle$ and the standard deviation $\Delta g = [\langle (g - \langle g \rangle)^2 \rangle]^{1/2}$ are plotted as a function of the wire length. (*b*) The standard deviation of $\ln(g)$ as a function of the wire length. The two straight lines represent the relations of $\Delta \ln(g) \propto L$ and $L^{1/2}$. The averages are calculated from 25 equivalent samples with $k_F W/\pi = 2.7$, $d/\lambda_F = 0.8$, and $\Delta/\lambda_F = 0.2$.

a Gaussian-like distribution of $\ln G$ in the strong-disorder limit. The root mean square deviation of the conductance is plotted in figure 7(*a*) as a function of the length of the wire. The conductance fluctuation increases rapidly as L is increased. When L exceeds the mean free path, we find that the fluctuation possesses the universal amplitude of $0.4 \sim 0.6e^2/h$ [3]. The root mean square deviation of $\ln(g)$ is plotted in figure 7(*b*). It has been suggested that $\Delta \ln(g)$ in general disordered system is given in the limiting cases as [29]

$$\Delta \ln(g) \propto \begin{cases} L/l_e & L/l_e \ll 1 \\ (L/l_e)^{1/2} & L/l_e \gg 1. \end{cases} \tag{9}$$

The numerical result shows a reasonable agreement with the analytical prediction.

Acknowledgments

This work was supported in part by the Office of Naval Research. The authors thank Qin Li for helpful suggestions.

Appendix. Scattering matrix for discontinuous junctions

In this appendix we derive the exact analytical form of the scattering matrix across discontinuous junctions. It is apparent that we need to treat two kinds of discontinuous junctions shown in figures A1(*a*) and A1(*b*). The mode-mixing parameters are obtained by using the mode-matching method. Let us first consider the 'wide–narrow' junction shown in figure A1(*a*). This junction often appears in the simulation of quantum point contacts and the solution is well known. The

wavefunction in each waveguide section is given by (2). Therefore, taking into account the orthonormal property of the eigenfunctions and the continuity condition for the wavefunction and the normal derivative at the junction, we get the following equations

$$\mathbf{K}_1^{-1}(\mathbf{E}_1 a_1 + b_1) = C\mathbf{K}_2^{-1}(a_2 + \mathbf{E}_2 b_2) \tag{A1a}$$

$$\mathbf{C}^{\mathrm{T}}\mathbf{K}_1(\mathbf{E}_1 a_1 - b_1) = \mathbf{K}_2(a_2 - \mathbf{E}_2 b_2) \tag{A1b}$$

where $\mathbf{K}_i$ and $\mathbf{E}_i$ are diagonal matrices given by

$$(\mathbf{K}_i)_{mn} = (k_m^{(i)})^{1/2}\delta_{mn} \tag{A2}$$

$$(\mathbf{E}_i)_{mn} = \exp(\mathrm{i}k_m^{(i)}d)\delta_{mn}. \tag{A3}$$

The matrix $\mathbf{C}$, which characterizes the mode-mixing, is defined by the overlap integral

$$(\mathbf{C})_{mn} = \int u_m^{(1)}(y)u_n^{(2)}(y)\,\mathrm{d}y. \tag{A4}$$

One readily obtains the scattering matrix

$$\mathbf{t} = 2(\mathbf{C}^{\mathrm{T}}\mathbf{K}_1^2\mathbf{C}\mathbf{K}_2^{-1} + \mathbf{K}_2)^{-1}\mathbf{C}^{\mathrm{T}}\mathbf{K}_1\mathbf{E}_1 \tag{A5a}$$

$$\mathbf{r}' = (\mathbf{C}^{\mathrm{T}}\mathbf{K}_1^2\mathbf{C}\mathbf{K}_2^{-1} + \mathbf{K}_2)^{-1}(\mathbf{K}_2 - \mathbf{C}^{\mathrm{T}}\mathbf{K}_1^2\mathbf{C}\mathbf{K}_2^{-1})\mathbf{E}_2 \tag{A5b}$$

$$\mathbf{r} = (\mathbf{K}_1^{-1} + \mathbf{C}\mathbf{K}_2^{-2}\mathbf{C}^{\mathrm{T}}\mathbf{K}_1)^{-1}(\mathbf{C}\mathbf{K}_2^{-2}\mathbf{C}^{\mathrm{T}}\mathbf{K}_1 - \mathbf{K}_1^{-1})\mathbf{E}_1 \tag{A5c}$$

$$\mathbf{t}' = 2(\mathbf{K}_1^{-1} + \mathbf{C}\mathbf{K}_2^{-2}\mathbf{C}^{\mathrm{T}}\mathbf{K}_1)^{-1}\mathbf{C}\mathbf{K}_2^{-1}\mathbf{E}_2. \tag{A5d}$$

The scattering matrix for the 'narrow–wide' junction is obtained by repeating a similar procedure.

In order to analyse the step discontinuity shown in figure A1(b), we introduce a fictitious wide waveguide section between the two sections as shown in figure A1(c). Considering the continuity conditions at the junctions and taking the limit $\epsilon \to 0$, one obtains the relations:

$$\mathbf{C}_1\mathbf{K}_1^{-1}(\mathbf{E}_1 a_1 + b_1) = \mathbf{C}_2\mathbf{K}_2^{-1}(a_2 + \mathbf{E}_2 b_2) \tag{A6a}$$

$$(\mathbf{C}_1^{\mathrm{T}})^{-1}\mathbf{K}_1(\mathbf{E}_1 a_1 - b_1) = (\mathbf{C}_2^{\mathrm{T}})^{-1}\mathbf{K}_2(a_2 - \mathbf{E}_2 b_2). \tag{A6b}$$

The matrices $\mathbf{C}_1$ and $\mathbf{C}_2$ are defined by the overlap integrals:

$$(\mathbf{C}_1)_{mn} = \int u_m^{(3)}(y)u_n^{(1)}(y)\,\mathrm{d}y \tag{A7a}$$

$$(\mathbf{C}_2)_{mn} = \int u_m^{(3)}(y)u_n^{(2)}(y)\,\mathrm{d}y. \tag{A7b}$$

Therefore, the scattering matrix is given by

$$\mathbf{t} = 2(\mathbf{C}_1\mathbf{K}_1^{-2}\mathbf{C}_1^{\mathrm{T}}(\mathbf{C}_2^{\mathrm{T}})^{-1}\mathbf{K}_2 + \mathbf{C}_2\mathbf{K}_2^{-1})^{-1}\mathbf{C}_1\mathbf{K}_1^{-1}\mathbf{E}_1 \tag{A8a}$$

$$\mathbf{r}' = (\mathbf{C}_1\mathbf{K}_1^{-2}\mathbf{C}_1^{\mathrm{T}}(\mathbf{C}_2^{\mathrm{T}})^{-1}\mathbf{K}_2 + \mathbf{C}_2\mathbf{K}_2^{-1})^{-1}(\mathbf{C}_1\mathbf{K}_1^{-2}\mathbf{C}_1^{\mathrm{T}}(\mathbf{C}_2^{\mathrm{T}})^{-1}\mathbf{K}_2 - \mathbf{C}_2\mathbf{K}_2^{-1})\mathbf{E}_2 \tag{A8b}$$

$$\mathbf{r} = (\mathbf{C}_2\mathbf{K}_2^{-2}\mathbf{C}_2^{\mathrm{T}}(\mathbf{C}_1^{\mathrm{T}})^{-1}\mathbf{K}_1 + \mathbf{C}_1\mathbf{K}_1^{-1})^{-1}(\mathbf{C}_2\mathbf{K}_2^{-2}\mathbf{C}_2^{\mathrm{T}}(\mathbf{C}_1^{\mathrm{T}})^{-1}\mathbf{K}_1 - \mathbf{C}_1\mathbf{K}_1^{-1}) \tag{A8c}$$

$$\mathbf{t}' = 2(\mathbf{C}_2\mathbf{K}_2^{-2}\mathbf{C}_2^{\mathrm{T}}(\mathbf{C}_1^{\mathrm{T}})^{-1}\mathbf{K}_1 + \mathbf{C}_1\mathbf{K}_1^{-1})^{-1}\mathbf{C}_2\mathbf{K}_2^{-1}\mathbf{E}_2. \tag{A8d}$$

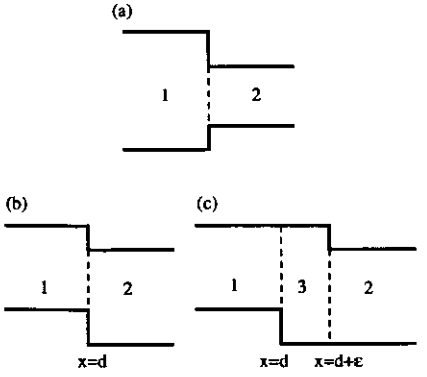

Figure A1. (*a*), (*b*) Discontinuous junctions in electron waveguides. In order to deal with the mode-matching across the junction shown in (*b*), we assume a fictitious waveguide section at the interface as shown in (*c*).

References

[1] See for example
Kirk W P and Reed M A (ed) 1992 *Nanostructures and Mesoscopic Systems* (New York: Academic)

[2] Washburn S and Webb R A 1986 *Adv. Phys.* **35** 375

[3] Lee P A, Stone A D and Fukuyama H 1987 *Phys. Rev.* B **35** 1039

[4] Hensel J C, Tung R T, Poate J M and Unterwald F C 1985 *Phys. Rev. Lett.* **54** 1840
Tešanović Z, Jarić M V and Maekawa S 1986 *Phys. Rev. Lett.* **57** 2760

[5] Sakaki H, Noda T, Hirakawa K, Tanaka M and Matsusue T 1987 *Appl. Phys. Lett.* **51** 1934

[6] Sakaki H 1980 *Japan. J. Appl. Phys.* **19** L735

[7] van Wees B J, van Houten H, Beenakker C W J, Williamson J G, Kouwenhoven L P, van der Marel D and Foxon C T 1988 *Phys. Rev. Lett.* **60** 848
Wharam D A, Thornton T J, Newbury R, Pepper M, Ahmed H, Frost J E F, Hasko D G, Peacock D C, Ritchie D A and Jones G A C 1988 *J. Phys. C: Solid State Phys.* **21** L209

[8] Roukes M L, Scherer A, Allen Jr S J, Craighead H G, Ruthen R M, Beebe E D and Harbison J P 1987 *Phys. Rev. Lett.* **59** 3011

[9] Hiramoto T, Hirakawa K, Iye Y and Ikoma T 1987 *Appl. Phys. Lett.* **51** 1620

[10] Laux S E, Frank D J and Stern F 1988 *Surf. Sci.* **196** 101

[11] Hamilton A R, Frost J E F, Smith C G, Kelly M J, Linfield E H, Ford C J B, Ritchie D A, Jones G A C, Pepper M, Hasko D G and Ahmed H 1992 *Appl. Phys. Lett.* **60** 2782

[12] Petroff P M, Gossard A C and Wiegman W 1986 *Appl. Phys. Lett.* **45** 620
Fukui T and Ando S 1989 *Electron. Lett.* **25** 410

[13] Thornton T J, Roukes M L, Scherer A and van de Gaag B P 1989 *Phys. Rev. Lett.* **63** 2128

[14] van Houten H, Beenakker C W J, van Wees B J and Mooij J E 1988 *Surf. Sci.* **196** 144

[15] Akera H and Ando T 1991 *Phys. Rev.* B **43** 11676

[16] Makarov N M and Yurkevich I V 1989 *Sov. Phys.–JETP* **69** 628 (Engl. Transl. 1989 *Zh. Eksp. Teor. Fiz.* **96** 1106)

[17] Cahay M, McLennan M and Datta S 1988 *Phys. Rev.* B **37** 10125

[18] Bandyopadhyay S and Cahay M 1991 *Computational Electronics* ed K Hess, J P Leburton and U Ravaioli (Boston: Kluwer) p 223

[19] Nixon J A, Davies J H and Baranger H U 1991 *Phys. Rev.* B **43** 12638

[20] Bagwell P F 1990 *Phys. Rev.* B **41** 10354

[21] Since we assume an equivalent length of waveguide sections, we include the phase shifts due to free propagation between junctions (see [17]) in the definition of the scattering matrix

[22] Landauer R 1957 *IBM J. Res. Dev.* **1** 223
Büttiker M, Imry Y, Landauer R and Pinhas S 1985 *Phys. Rev.* B **31** 6207
Imry Y 1986 *Directions in Condensed Matter Physics* ed G Gristein and G Mazenko (Singapore: World Scientific) p 101

[23] Anderson P W, Thouless D J, Abrahams E and Fisher D S 1980 *Phys. Rev.* B **22** 3519

[24] Kander I, Imry Y and Sivan U 1990 *Phys. Rev.* B **41** 12941

[25] Chu C S and Sorbello R S 1989 *Phys. Rev.* B **40** 5941

[26] Pichard J L and Andre G 1986 *Europhys. Lett.* **2** 477

[27] Imry Y 1985 *Europhys. Lett.* **1** 249
[28] Takagaki Y and Ferry D K 1992 *Phys. Rev.* B **45** 13494
[29] Abrikosov A A 1981 *Solid State Commun.* **37** 997